

# S-Adenosylmethionine Inhibits the Proliferation of Retinoblastoma Cell Y79, Induces Apoptosis and Cell Cycle Arrest of Y79 Cells by Inhibiting the Wnt2/ $\beta$ -Catenin Pathway

Mushi Liu<sup>1</sup> · Youchaou Mobet<sup>2</sup> · Hong Shen<sup>1,3</sup>✉

## Abstract

Retinoblastoma is one of the most common primary intraocular malignancies in young children. Traditional treatment methods such as chemotherapy often come with significant adverse effects, such as hearing loss, cognitive impairment, and vision loss. Therefore, there is an urgent need to explore a novel therapeutic drug that is both effective and safe. S-adenosylmethionine (SAM) is a natural compound known to exhibit anti-proliferative effects in various cancer cell lines. However, to date, no studies investigated the effects of SAM on retinoblastoma cells and its potential mechanisms of action. Therefore, this study aims to investigate the impact of SAM on retinoblastoma cells and explore its possible mechanisms of action, with the hope of providing new insights into the treatment of this disease. The optimal concentration of SAM was determined using the Cell Counting Kit-8 assay. The effect of SAM on retinoblastoma proliferation was assessed using the 5-ethynyl-2'-deoxyuridine cell proliferation assay. Y79 cells were subjected to hematoxylin and eosin stain and electron microscopy to observe any morphological changes induced by SAM. The stages of SAM's action on the retinoblastoma cell cycle and its apoptotic effects were measured using flow cytometry. The apoptotic effect of SAM on retinoblastoma was further confirmed using the TUNEL assay. Differential expression of related genes was detected through RT-PCR. *In vivo* subcutaneous tumor formation in nude mice and immunohistochemistry were employed to validate the effect of SAM on retinoblastoma-related phenotypes. Western blotting was conducted to investigate whether SAM modulated retinoblastoma-related phenotypes via the Wnt2/ $\beta$ -catenin pathway. SAM arrested the cell cycle of retinoblastoma at the G1 phase, induced apoptosis of retinoblastoma cells through the Wnt2/ $\beta$ -catenin pathway, and affected their morphology and even ultrastructure. In addition, *in vitro* and *in vivo* experiments demonstrated that SAM had an oncogenic effect on retinoblastoma. In this study, we verify *in vitro* and *in vivo* whether SAM inhibits the proliferation of retinoblastoma cell Y79, induces apoptosis and cell cycle arrest of Y79 cells by inhibiting the Wnt2/ $\beta$ -catenin pathway, and affects the morphology and structure of retinoblastoma cell Y79.

## Keywords

Retinoblastoma · S-adenosylmethionine · Wnt2/ $\beta$ -catenin · Y79

Received: 24 April 2024 / Accepted: 5 August 2024/

© L. Hirszfeld Institute of Immunology and Experimental Therapy, Wrocław, Poland 2024

## Abbreviations

CCK8, Cell counting kit-8; EDU, 5-Ethynyl-2'-deoxyuridine; H&E, Hematoxylin and eosin stain; SAM, S-adenosylmethionine.

## 1. Introduction

Retinoblastoma is indeed a serious and challenging condition that affects young children. Retinoblastoma, a malignant tumor mainly impacting the retina, which is the light-sensitive tissue located at the back of the eye. In recent years, various treatment options have emerged, offering alternatives to eye removal. Conservative therapies like chemical volume reduction, transpupillary thermotherapy, cryotherapy, laser photocoagulation, and radiotherapy have shown promise in preserving the eye and vision. Additionally, advancements in genetics, interventions, and traditional Chinese medicine have contributed to the evolving field of retinoblastoma treatment (Yan et al. 2021). In the last 30 years, approximately

42% of patients have had their eyes removed, and 12% have lost their lives as a result of retinoblastoma (Luo et al. 2022). While these advancements are encouraging, it is important to acknowledge that the overall survival rate of retinoblastoma patients remains low (Dimaras et al. 2015). Challenges such as blindness continue to impact patients, highlighting the need for further research, improved treatments, and increased awareness. Medical professionals, researchers, and policymakers need to work together to enhance early detection methods, develop more effective treatments, and offer essential assistance to enhance the prognosis and enhance the quality of life for individuals with retinoblastoma in China and globally (Pascual-Pasto et al. 2019).

Indeed, S-adenosylmethionine (SAM) is a vital biomolecule within mammalian cells. Its significance lies in its involvement in essential metabolic pathways such as transmethylation, transsulfuration, and aminopropylation pathways. SAM has been utilized as a prophylactic medication for the treatment of mood disorders, fibromyalgia, joint pain, intrahepatic cholestasis (Vincenzi et al. 2018), and alcoholic liver disease (Lu et al. 2020). Furthermore, urine SAM levels have been identified as a noninvasive biomarker for monitoring the decline of renal function in

<sup>1</sup> Medical College, South China University of Technology, Guangzhou, China

<sup>2</sup> Bai Sheng Biological Products Co., Ltd, Guangzhou, China

<sup>3</sup> Department of Pathology, School of Basic Medical Sciences, Southern Medical University, China

✉ shenhong2010168@163.com; Heshujie1388@163.com

the early stages of chronic renal disease (Kruglova et al. 2021). SAM is indeed involved in various cellular processes beyond its main role as a methyl donor. It has great importance in regulating cell proliferation, apoptosis, metastatic invasion, and the cell cycle (Parashar et al. 2015; Hayashi et al. 2018). SAM has demonstrated inhibitory effects on osteosarcoma cells, tumor metastasis, breast cancer (Mahmood et al. 2020), gallbladder cancer (Liu et al. 2020), colon cancer (Zsigrai et al. 2020), and more.

The Wnt/ $\beta$ -catenin signaling pathway is a highly conserved intracellular signal transduction pathway that significantly influences a range of biological processes, including the regulation of cell adhesion, proliferation, apoptosis, and inflammatory responses (Perugorria et al. 2019). Abnormal expression of this pathway has been implicated in tumorigenesis and tumor development (Spitzner et al. 2021). For instance, the activation of the Wnt/ $\beta$ -catenin pathway by AXIN1 has been shown to promote the progression of gastric cancer. In gliomas, dysregulation of this pathway contributes to the clinical malignancy and prognosis of patients (Bai et al. 2017; He et al. 2019). Furthermore, the potential therapeutic targeting of the Wnt/ $\beta$ -catenin pathway by IGF2BP1 and its role as a predictive marker for colon cancer is being actively explored. This could enhance the accuracy of colon cancer diagnosis and potentially reduce the costs associated with detection and treatment (Singh et al. 2023).

We are conducting further experiments to explore the mechanisms by which SAM influences retinoblastoma. Dysregulation of the Wnt/ $\beta$ -catenin signaling pathway, which is recognized for its involvement in cellular proliferation, differentiation, and apoptosis, has been linked to various cancers, including retinoblastoma. We can potentially discover new targets for clinical treatment by investigating whether SAM affects the proliferation, apoptosis, and other cellular processes of retinoblastoma through the Wnt/ $\beta$ -catenin signaling pathway. Furthermore, by studying whether SAM could reduce the expression of the Wnt/ $\beta$ -catenin protein signaling pathway, we can potentially uncover valuable information regarding its therapeutic potential. Overall, our research can establish a novel theoretical foundation for the clinical management of retinoblastoma and contribute to our comprehension of the molecular mechanisms underlying this disease.

## 2. Materials and Methods

All experiments involving mice were approved by the Animal Centre of the Medical College of South China University of Technology (ethical number: 2023105). SAM (Coolaber, China; Dissolved in ultrapure water); HLY78 (HY-122816, Med Chem Express, USA).

### 2.1. Cell culture

Retinoblastoma Y79 (Shanghai Zhongqiao Xinzhou, China,  $N \leq 15$ ) was cultured in RPMI-1640 medium (BI, Israel) supplemented with 20% fetal bovine serum (FBS; BI) and 1% penicillin-streptomycin. ARPE-19 (Shanghai Zhongqiao Xinzhou,  $N \leq 15$ ) was cultured in a DMEM/F12 medium (Gibco, USA) containing 10% FBS and 1% penicillin-streptomycin. Both cell types were maintained at 37°C in a CO<sub>2</sub> incubator with a concentration of 5% CO<sub>2</sub>.

### 2.2. Cell counting kit-8 (CCK8) assay

Y79 (5000 cells per well) were cultured in 96-well plates containing 100  $\mu$ L of growth medium. Y79 cells were treated with different concentrations of SAM (ranging 0–2.4 mM) for various time points (24 h, 48 h, and 72 h), ARPE-19 (3000 cells per well) cells for 72 h. All wells were incubated with 10  $\mu$ L CCK8 and incubated continuously at 37°C for 2 h. Absorbance was measured at 450 nm using an ELISA reader. The reported results represent the mean values obtained from at least three independent wells.

### 2.3. 5-Ethynyl-2'-deoxyuridine (EDU) cell proliferation assay

Single-cell suspension was prepared from Y79 cells in the logarithmic growth phase and inoculated in 12-well plates. After adding SAM 1 mM and 2 mM for 48 h, 2 $\times$  of EdU working solution (20  $\mu$ M), pre-warmed at 37°C, was added in equal volume to each well, and continued to be incubated for 5.5 h at 37°C, 5% CO<sub>2</sub> cell culture box. Immunofluorescence staining was performed according to the instructions of BeyoClick™ EdU-594 Cell Proliferation Detection Kit (Beyotime, China), and finally blocked by adding an anti-fluorescence quencher containing DAPI. The cells were observed under a fluorescence microscope (Zeiss, Germany), and three fields of view were randomly selected. The cell proliferation rate was equal to EDU-positive cells/DAP-positive cells. The cell proliferation rate of the three fields was taken as the mean.

### 2.4. Hematoxylin and eosin stain (H&E)

Logarithmic growth phase Y79 cells were prepared as single-cell suspension. The cell concentration was adjusted to  $1 \times 10^6$  cells/mL. Approximately 2–3 drops (about 30–50  $\mu$ L) of the cell suspension were evenly smeared onto autoclaved glass slides. The slides were air-dried for 10 min at room temperature, followed by washing with phosphate-buffered saline (PBS) for 3 min  $\times$  3 times. The cells were fixed in 95% ethanol for 10–15 min, and then washed with PBS 3 times, each

for 3 min. Subsequently, the slides were rinsed with deionized water once for 3 min. Staining was carried out using hematoxylin for 3 min, followed by a quick rinse with running water for 3 s. Differentiation was achieved by treating the slides with 1% hydrochloric acid ethanol for 10 s, and then counterstained with eosin for 4 min. Dehydration was performed using a series of ethanol gradients (75%, 80%, 90%, 95%, 95%, 100%, 100%) for 1 min each. The slides were cleared in xylene I and II and mounted with neutral mounting medium. Images were scanned and observed using Digital Pathology Scanner (Leica, Germany). Three random fields were selected. To determine the mitotic index, we calculated the ratio of the number of mitotic cells to the total number of cells.

### 2.5. Electron microscopy

The samples were quickly and accurately intercepted and then fixed overnight in 2.5% glutaraldehyde. Rinsed with 0.1 M phosphoric acid rinse solution 3 times for 15 min each time. Fixed the samples in 1% osmium acid for 2 h at 4°C in a refrigerator and washed with ultrapure water 3 times for 15 min each time. Gradient dehydration followed by embedding was placed in a constant temperature oven for polymerization, slices (70 nm) were cut using an ultrathin sectioning machine (Leica), and 3% uranyl acetate-lead citrate was double-stained and then visualized under a transmission electron microscope (Hitachi, Japan) and photographed.

### 2.6. Flow cytometry cell cycle analysis

Harvested Y79 cells were washed twice with pre-cooled PBS and then fixed in 70% ice-cold ethanol at -20°C overnight. The ethanol was removed by centrifugation and the precipitate was resuspended in 1× PBS. The cells were resuspended in 0.5 mL of Staining Solution, which was prepared by adding 100 µL of RNase A solution and 200 µL of Nuclear Dye to 10 mL of 1× Assay Buffer. The cell suspension was then incubated in the dark at 37°C for 30 min. The cells were washed twice with PBS and resuspended. Cells were analyzed within 48 h on a high-end analytical flow cytometer (BD LSRFortessa Configuration Penta-Laser 18-Colour System, USA) using the appropriate channel (Ex/Em = 535/615 nm), data were analyzed by FlowJO 10.8.1 software (Becton, Dickinson and Company, USA).

### 2.7. Flow cytometry apoptosis assay

In this study, apoptosis was detected using Annexin V-AbFluor 488/PI Double Staining Apoptosis Detection Kit (Abbkine, Wuhan, China). Briefly, Y79 cells and different concentrations (1 mmol/L and 2 mmol/L) of SAM-treated Y79 cells ( $3 \times 10^5$  cells/well) were grown in 6-well plates.

After 48 h of incubation, the supernatant was discarded, and the cells were rinsed with pre-cooled PBS and then resuspended with 1× Binding buffer. Subsequently, 5 µL of Annexin V-fluorescein isothiocyanate (V-FITC) and 2 µL of propidium iodide (PI) were added to the cell suspension, mixed homogeneously, and incubated at room temperature for 15 min under light. Finally, the apoptosis rate was assessed via flow cytometry within 1 h, in accordance with the instructions provided in the kit.

### 2.8. TUNEL experiments

According to the instructions of TUNEL Apoptosis Detection Kit (green fluorescence, Abbkine, Wuhan, China), Y79 (about  $1 \times 10^6$  cells/mL) was treated with different concentrations (1 mmol/L and 2 mmol/L) of SAM for 48 h. The supernatant was removed, washed twice with PBS, fixed with 4% paraformaldehyde, washed again and permeabilized, and then stained in the dark at 37°C with TUNEL reagent for 1 h, and photographed with an orthogonal fluorescence microscope (Zeiss) with three randomly selected fields of view. The apoptotic index was equal to TUNEL-positive cells/DAPI-positive cells. The apoptotic index of the three fields was taken as the mean.

### 2.9. RT-PCR experiments

Pre-treated cellular RNA was extracted using Trizol reagent (TIANGEN, China), and RNA (10 µg) from each sample was reverse transcribed using PrimeScript RT Master Mix (Perfect Real Time) (Takara, Japan). TB Green Premix Ex Tag II (Tli RNaseH Plus) was used for PCR, and each real-time PCR was performed on a real-time fluorescent quantitative PCR instrument (BIO-RAD, USA) with three replicate wells per group, totaling 25 µL of reaction mixture. Relative expression of Ki67, CASPASE 3, BAX, BCL-2, MMP-2, MMP-9, VEGF, TGF-β, cycD, P21, TP53, Wnt2, β-CATENIN, cycD, c-MYC c-JUN, Axin, and GSK-3β were normalized to GAPDH respectively. The primers were as follows (Table 1):

### 2.10. Western blot

Y79 cellular proteins were extracted in a mixture of RIPA lysate (Beyotime) and 2% phosphatase protease (Beyotime) for 30 min on ice. The extracts were centrifuged at 14,000×g for 15 min at 4°C and the supernatant was collected. Protein concentration was quantified using the BCA Protein Assay Kit (Beyotime). Proteins (20 µg) were separated by SDS-PAGE and transferred onto a polyvinylidene difluoride membrane. The membranes were sealed in a rapid closure solution and incubated for 20 min at room temperature. Subsequently, they were incubated overnight at 4°C with the primary antibodies: Wnt2 (ER1511-4, 1:2000, Huaan Bio, China),

**Table 1.** The primers of RT-PCR

| Genes            | Primer sequences  |
|------------------|---|
| <i>GAPDH</i>     | F: 5'-ACCCACTCCTCCACCTTTGAC-3'<br>R: 5'-TGTTGCTGTAGCCAAATTCGTT-3'         |
| <i>Ki67</i>      | F: 5'-ACGCCTGGGTACTATCAAAAGG-3'<br>R: 5'-CAGACCCATTACTTGTGTTGGA-3'        |
| <i>CASPASE 3</i> | F: 5'-GAAATTGTGGAATTGATGCGTGA-3'<br>R: 5'-CTACAACGATCCCTCTGAAAAA-3'       |
| <i>Bax</i>       | F: 5'-CCCGAGAGGTCTTTTCCGAG-3'<br>R: 5'-CCAGCCCATGATGGTTCTGAT-3'           |
| <i>BCL-2</i>     | F: 5'-GGTGGGGGTCATGTGTGTGG-3'<br>R: 5'-CGGTCAGTACTCAGTCATCC-3'            |
| <i>MMP-2</i>     | F: 5'-CCCACTGCGGTTTTCTCGAAT-3'<br>R: 5'-CAAAGGGGGTATCCATCGCCAT-3'         |
| <i>MMP-9</i>     | F: 5'-TGTACCGCTATGGTACACTCG-3'<br>R: 5'-GGCAGGGGACAGTTGCTTCT-3'           |
| <i>VEGF</i>      | F: 5'-AGGGCAGAATCATCAGAAGT-3'<br>R: 5'-AGGGTCTCGATTGGATGGCA-3'            |
| <i>TGF-β</i>     | F: 5'-CTAATGGTGAAACCCACAACG-3'<br>R: 5'-TATCGCCAGGAATTGTTGCTG-3'          |
| <i>P21</i>       | F: 5'-CGATGGAAGTTCGACTTTGTCA-3'<br>R: 5'-GCACAAGGGTACAAGACAGTG-3'         |
| <i>TP53</i>      | F: 5'-GAGGTTGGGCTCTCTGACTGTACC-3'<br>R: 5'-TCCGTCCCAGTAGATTACCAC-3'       |
| <i>β-CATENIN</i> | F: 5'-CCTGTTCCCTGAGGGTATT-3'<br>R: 5'-CCATCAAATCAGCTTGAGTAGCC-3'          |
| <i>Wnt2</i>      | F: 5'-GCCTTTGTTTATGCCATCTCCT-3'<br>R: 5'-CTTGCGCTTCCCATCTTCTT-3'          |
| <i>c-MYC</i>     | F: 5'-TGCACCCACATCATCTACAG-3'<br>R: 5'-ACTCGTCATTCCACTCCCAT-3'            |
| <i>cycD</i>      | F: 5'-AGTGAGCTCAGGAGGAGGTGGTGTA-3'<br>R: 5'-AGTAAGCTTGTGAGGGCAGAGGTGTC-3' |
| <i>c-JUN</i>     | F: 5'-TCCAAGTGCCGAAAAGGAAG-3'<br>R: 5'-CGAGTTCTGAGCTTTCAAGGT-3'           |
| <i>Axin1</i>     | F: 5'-GACAAGATCGCAGAGGAAGG-3'<br>R: 5'-ACCCCCACAGTCAAACTCGTC-3'           |
| <i>GSK-3β</i>    | F: 5'-CCTGGGAACTCCAACAAGGG-3'<br>R: 5'-GGGGTCGGAAGACCTTAGTC-3'            |

β-catenin (0407-16, 1:2000, Huaan Bio), Tubulin (66031-1-Ig, 1:5000, Proteintech, China), Caspase-3/Cleaved Caspase-3 (WL02117, 1:500, WanLei, China). After incubation with a secondary antibody, the blot was visualized by enhanced chemiluminescence (Beyotime) method. The intensity of positive blots was tested by Image J software (National Institutes of Health, Germany).

## 2.11. Animal experiment

To assess the impact of SAM on the growth of Y79 cells, a retinoblastoma xenograft model was established with 18 female BALB/c nude mice, aged 6 weeks, which were obtained from the Experimental Animal Centre of South China University of Technology. A Y79 cell suspension ( $8 \times 10^6$  cells) mixed with a 1:1 ratio of PBS and matrix gel was injected into the right side of the posterior flank of each mouse. Tumors were allowed to grow until reaching a volume of 200–500 mm<sup>3</sup>, at which point they were randomly allocated into three groups, with each group comprising six mice: (1) Control-0mM (0 mM SAM: sterile physiological saline), (2) SAM-1mM (40 mg/kg), (3) SAM-2mM (80 mg/kg). The mice in the SAM-treated groups received intraperitoneal injections of SAM (at either 40 mg/kg or 80 mg/kg) or an equivalent volume of saline 5 times, with a 2-day interval between each administration. During the experiment, the tumor volumes (calculated using the formula: Volume = (length × width<sup>2</sup>)/2) and the body weights of the mice were measured at regular intervals. After the final administration (1 day after tumor cell injection), the mice were euthanized, and the tumors were collected and weighed. All animal experiments were conducted according to the guidelines established by the Laboratory Animal Care and Use Committee of the School of Medicine, South China University of Technology.

## 2.12. Immunohistochemistry

The exfoliated tumors were fixed with 4% paraformaldehyde, embedded in paraffin, processed into tissue blocks, and sectioned into 4 μm-thick slices. These sections were then subjected to immunohistochemical analysis for cell proliferation marker Ki67 (27309-1-AP, 1:100, Proteintech) using the Rabbit Secondary Anti HRP Immunohistochemistry Kit (Zhongshan Jinqiao, China), following the kit's instructions.

## 2.13. Statistical analysis

All experiments were repeated at least 3 times. Data are presented as mean ± standard deviation from three independent experiments. Differences between three or more groups were analyzed using one-way analysis of variance (ANOVA). GraphPad Prism 9 (GraphPad, USA) was used to analyze statistical significance. *P*-values <0.05 were considered to indicate statistically significant results.

## 3. Results

### 3.1. SAM treatment suppressed the viability and proliferation of Y79 cells

Cancer cells are characterized by uncontrolled tumor cell growth resulting from dysregulated cell proliferation. Targeted



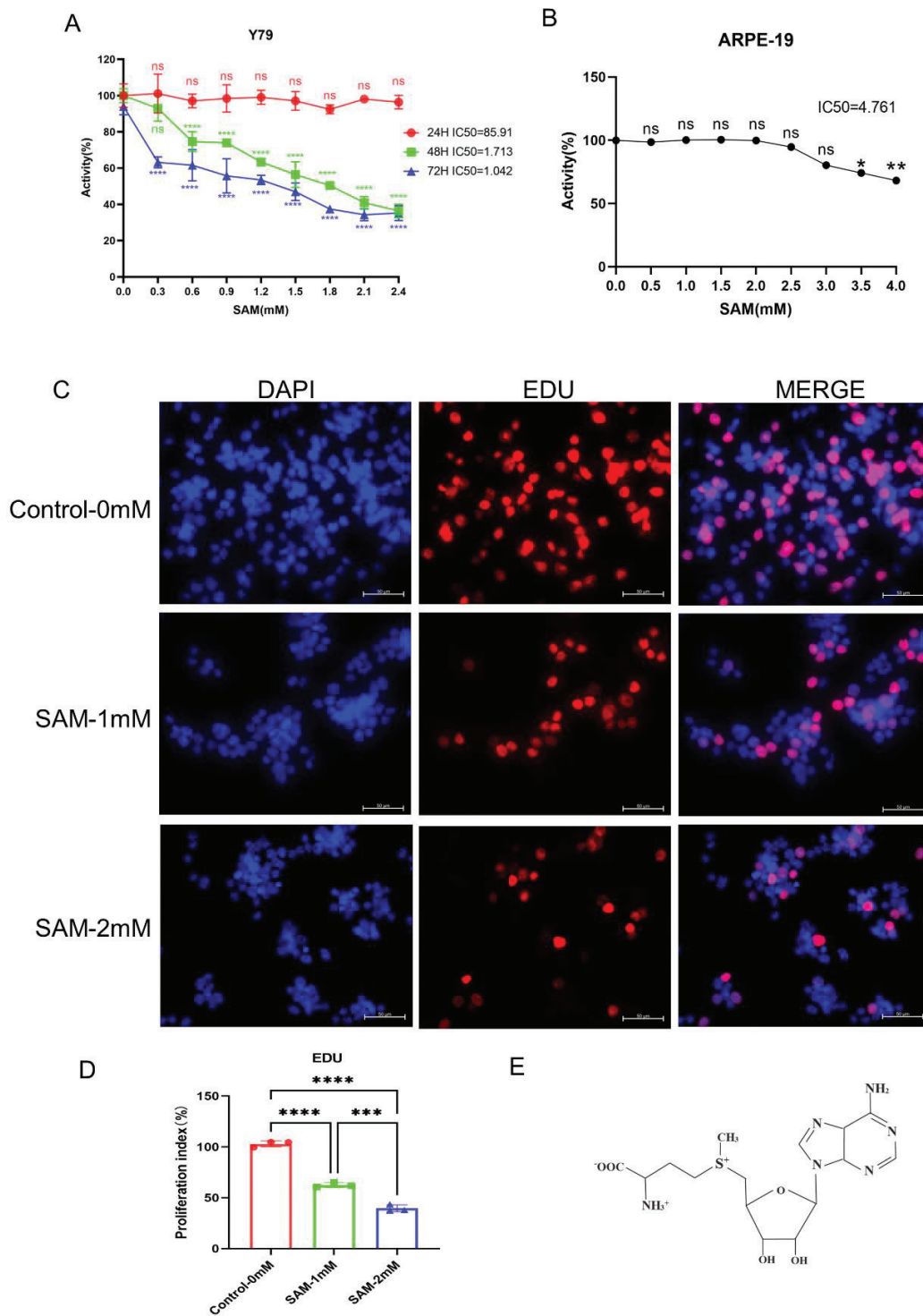


**Fig 1.** SAM inhibited cell viability and proliferation of Y79 cells. **(A)** CCK8 assay was conducted to test the effect of SAM on Y79 cell viability. **(B)** CCK8 assay was conducted to test the effect of SAM on ARPE-19 cell viability. **(C and D)** EDU experiment was used to verify the effect of SAM (1 mM, 2 mM) on cell proliferation. **(E)** The molecular structure of SAM was shown. Each experiment was repeated 3 times independently, and the data are presented as mean  $\pm$  standard deviation. Data in panels were analyzed using one-way ANOVA, nsP > 0.05, \*P < 0.05, \*\*P < 0.01, \*\*\*P < 0.001, \*\*\*\*P < 0.0001 (vs. control or low dose administration group). ANOVA, analysis of variance; CCK8, Cell counting kit-8; EDU, 5-Ethynyl-2'-deoxyuridine; SAM, S-adenosylmethionine.

containment of cell proliferation has been a significant focus in tumor therapeutics. Therefore, we first investigated the effect of SAM on the viability of Y79. First, Y79 cells were treated with different concentrations of SAM for 24 h, 48 h, and 72 h. The results showed that SAM was able to inhibit the viability of Y79 cells in a dose-dependent and time-dependent manner, and the IC<sub>50</sub> of Y79 cells after 48 h of treatment

was 1.713. The data presented in Figure 1a demonstrate that SAM exhibited a dose-dependent and time-dependent reduction in the viability of Y79 cells ( $P < 0.001$ ). Therefore, further two doses of SAM: 1 mM and 2 mM, and 48 h duration of action were chosen to treat the next experiments. Also to determine whether SAM adversely affects the viability of normal non-tumor cells, retinal epithelial cells ARPE-19

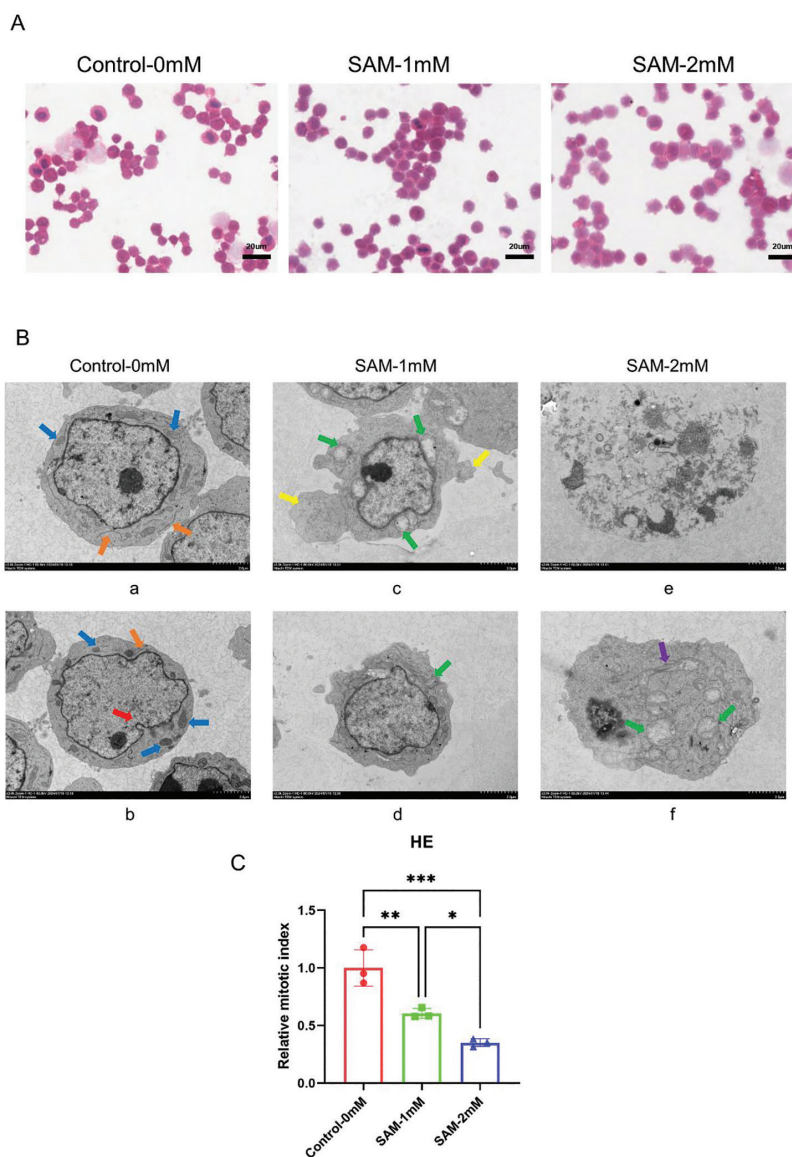


**Fig 2.** SAM affects the morphology of retinoblastoma cell lines and their ultrastructure. (A–C) Effect of SAM on the morphology of Y79 cells, with a concentration-dependent decrease in nuclear schizoprenic images. (b): Electron microscopic changes in the ultrastructure of retinoblastoma with changes in SAM concentration (12,000×). Control-0mM (a and b): Normal structure of retinoblastoma Y79 cells under transmission electron microscopy. SAM-1mM (Low-dose treatment group: [c and d]): Ultrastructural changes in retinoblastoma Y79 cells. SAM-2mM (high-dose treatment group: [e and f]): Ultrastructural changes in retinoblastoma Y79 cells. Red arrows indicate nuclear grooves, blue arrows denote normal mitochondria, orange arrows represent normal endoplasmic reticulum, yellow arrows point to apoptotic bodies, green arrows indicate swollen, ruptured, vacuolated mitochondria, and purple arrows denote swollen endoplasmic reticulum. Each experiment was repeated for 3 times independently, and the data are presented as mean  $\pm$  standard deviation. Data in panels were analyzed using one-way ANOVA, ns  $P > 0.05$ , \* $P < 0.05$ , \*\* $P < 0.01$ , \*\*\* $P < 0.001$  (vs. control or low dose administration group). ANOVA, analysis of variance; H&E, Hematoxylin and eosin stain; SAM, S-adenosylmethionine.

were treated with different concentrations of SAM for 72 h. Figure 1b shows that there was no toxic effect on ARPE-19 at SAM concentrations of 1 mM and 2 mM. After treating Y79 cells with both doses of SAM, 1 mM and 2 mM, for 48 h, the results from the EDU assays (Figures 1c and d) indicated that the proliferation of Y79 cells decreased in a concentration-dependent manner with increasing concentrations of SAM ( $P < 0.001$ ).

In order to investigate the effect of SAM on the morphology of retinoblastoma, first, in H&E staining, it was observed that the ratio of nuclear division of Y79 cells in the field decreased with the increase of SAM concentration (Figures 2a–c;  $P < 0.05$ ). Its effect on the ultrastructure of retinoblastoma was observed under the electron microscope, and the electron microscope results showed the following: (1) Control-0mM: retinoblastoma cells were smaller in size and had a high nucleoplasmic

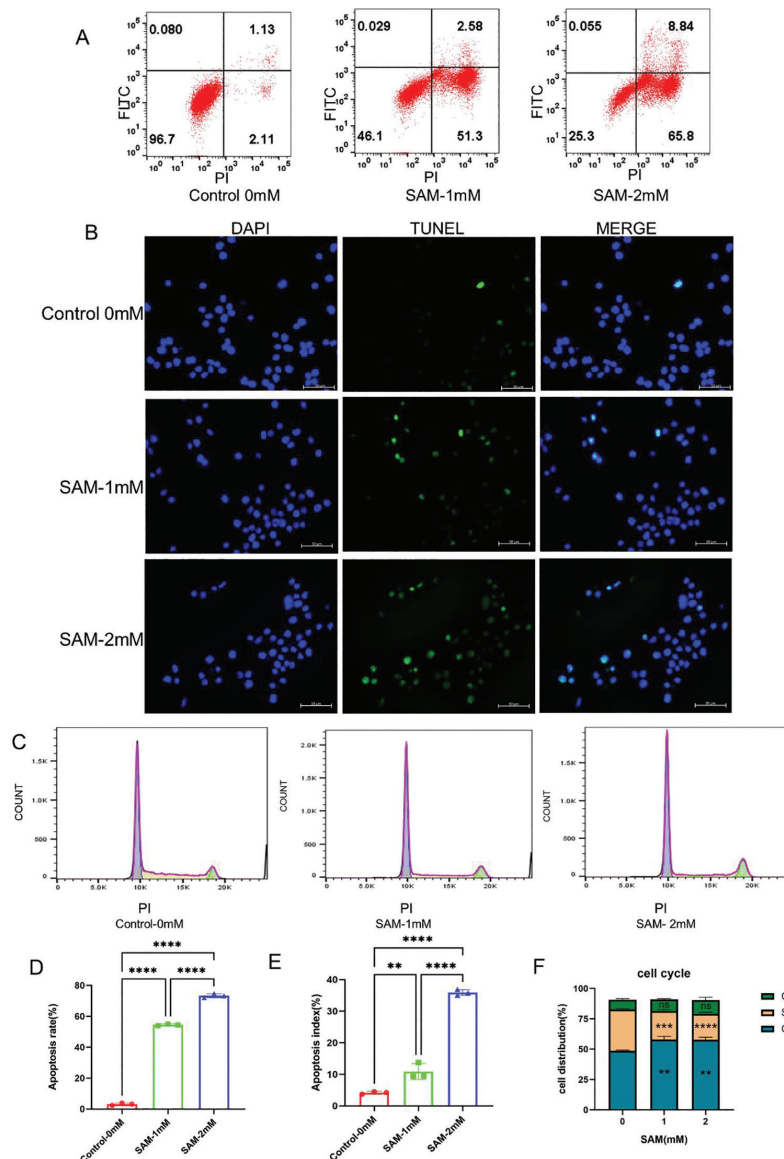


**Fig 3.** SAM inducing apoptosis and cell cycle arrest of Y79 cells were treated with SAM (1 mM, 2 mM) for 48 h. (A–D) Flow cytometry was used to test the effect of SAM on apoptosis. (B–E) TUNEL assay was carried out to detect the effect of SAM on apoptosis again. (C–F) Flow cytometry was used to test distribution of the apoptotic cells. The percentage of early and late apoptotic cells was assessed and compared to control group. The quantification of the data shows a significant increase of early and late apoptotic cells and a decrease of living cells after 48 h of treatment.  $N = 3$ . Each experiment was repeated for 3 times independently, and the data are presented as mean  $\pm$  standard deviation. Data in panels a–c were statistically analyzed by the using one-way ANOVA.  $nsP > 0.05$ ,  $^{**}P < 0.01$ ,  $^{****}P < 0.0001$  (vs. control or low dose administration group). ANOVA, analysis of variance; SAM, S-adenosylmethionine.

ratio. The nuclei were irregularly rounded under electron microscopy (the nuclei were rounded under light microscopy), and the surface area of the nuclei would be larger with nuclear grooves (Figure 2b). Overall, there are fewer organelles, mostly mitochondria and endoplasmic reticulum. The mitochondria were fewer in number and sparsely distributed; the endoplasmic reticulum was less developed and more heterogeneously altered with single, scattered flat vesicles (Figures 2a and b). (2) SAM-1mM: the chromatin of the tumor cells was densely packed and distributed along the nuclear membrane, and the nuclear membrane was wrinkled (Figures 2b–d). The overall cellular morphology was changed, with the appearance of apoptotic vesicles wrapped around cytoplasmic contents (e.g., endoplasmic reticulum) and nuclear material, and the mitochondrial cristae were fractured or even disintegrated (Figures 2b and c). (3) SAM-2mM: most of the tumor cells no longer had normal morphological structure and were completely destroyed, cells disintegrated and fragmented, and organelles were released (Figures 2b–e).

More apoptotic vesicles, and mitochondria were vacuolated or completely enlarged, and the endoplasmic reticulum was edematous (Figures 2b–f).

### 3.2. SAM treatment induced apoptosis and cell cycle arrest at G1 phase in Y79 cells

Apoptosis of Y79 cells was quantified using flow cytometry by detecting apoptosis by the membrane-linked protein V-FITC/PI binding assay after SAM treatment for 48 h. After treatment with 1 mM and 2 mM SAM, the apoptosis rate observed in the experimental groups was significantly higher compared to the control group (3.16%;  $P < 0.0001$ ). As shown, the mean apoptosis rates of Y79 cells after SAM-1mM and 2 mM SAM treatment were 54.51% and 73.33%, respectively, which were significantly higher compared to the control group (Figures 3a–d). These data suggest that SAM treatment dose-dependently induced apoptosis in Y79 cells.

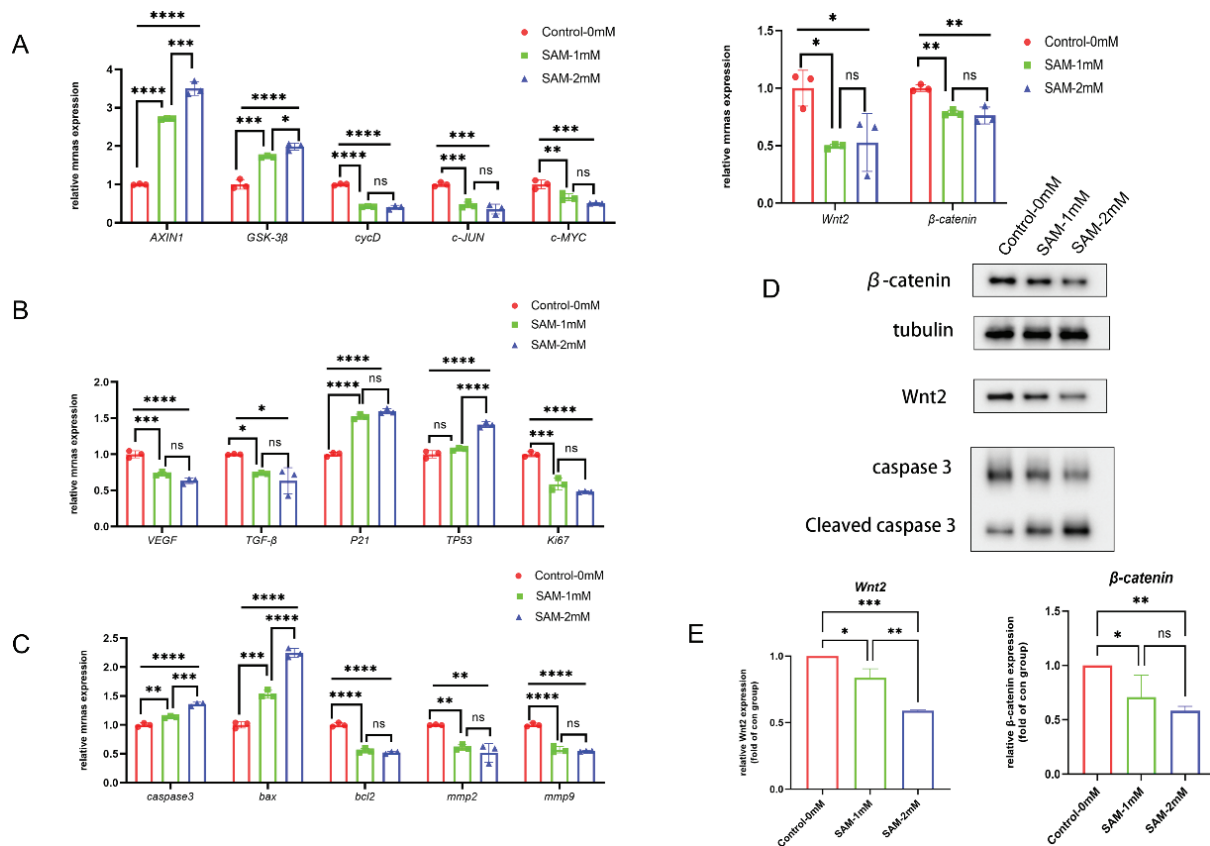


**Fig 4.** SAM treatment downregulated the expression of genes associated with the Wnt2/β-catenin signaling pathway in Y79 cells. Y79 cells were treated with SAM (1 mM, 2 mM) for 48 h. (A): RT-PCR was used to assess the impact of SAM on the mRNA levels of Wnt2, Axin1, β-catenin, c-MYC, cyclin D, c-JUN, and GSK-3β genes. (B and C): RT-PCR was employed to test the effect of SAM on the mRNA level of cell proliferation gene Ki67, metastasis-related genes P21, TP53, cell cycle-related genes mmp-2, mmp-9, cell cycle-related genes P21, TP53, vascular endothelial factor VEGF, TGF-β, apoptosis-related genes caspase3, bax, bcl-2. (D and E) Western blot analysis was performed to evaluate the protein levels of Wnt2 and β-catenin. The experiments were conducted with a sample size of N = 3 and repeated independently 3 times. The data are presented as mean ± standard deviation. nsP > 0.05, \*P < 0.05, \*\*P < 0.01, \*\*\*P < 0.001, \*\*\*\*P < 0.0001 (vs. control or low dose administration group). SAM, S-adenosylmethionine; TGF-β, transforming growth factor-β.



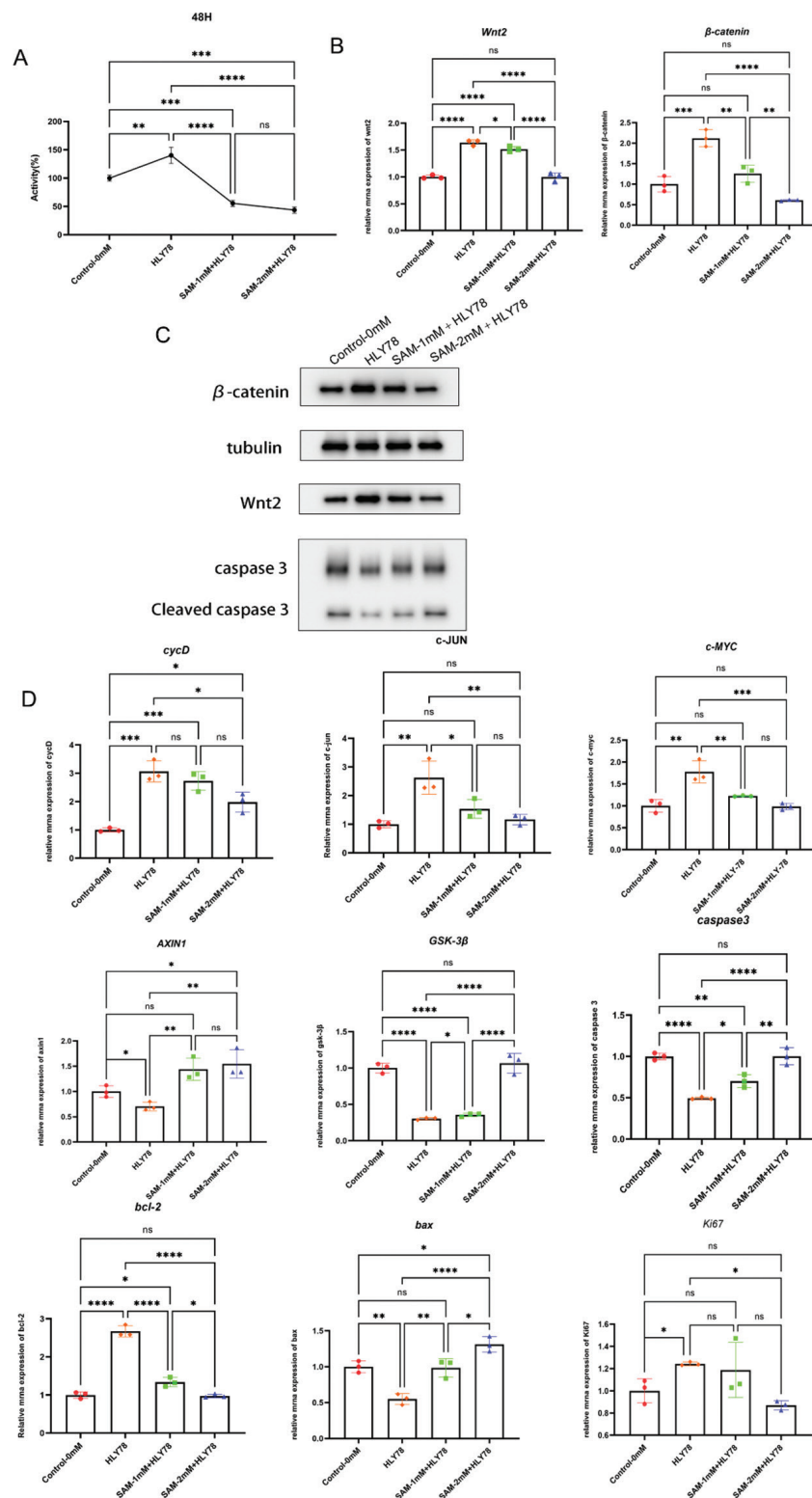
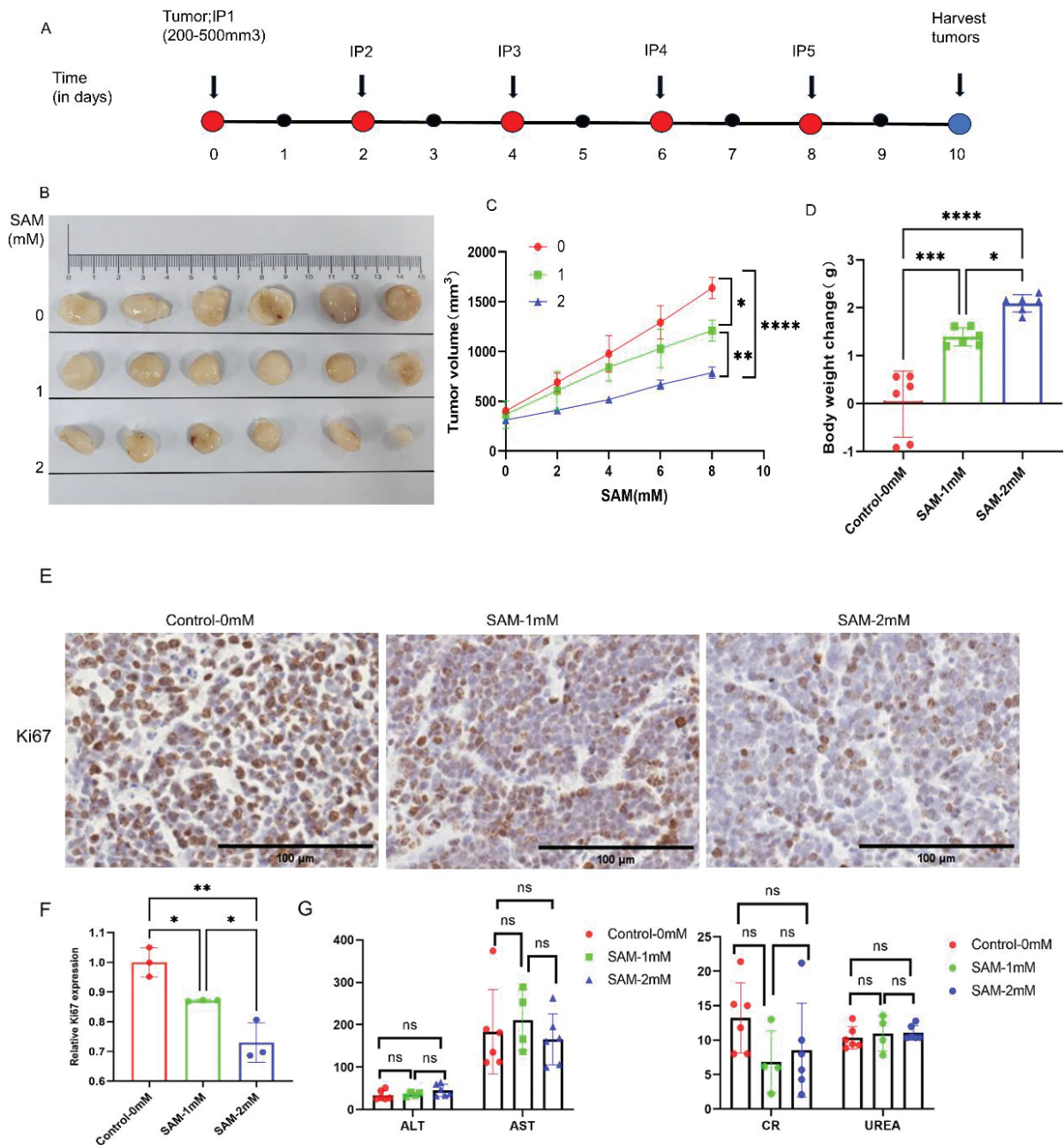


**Fig 5.** SAM attenuated the cancer-promoting effects induced by activation of the Wnt2/ $\beta$ -catenin signaling pathway (concentration-dependent attenuation). (A) CCK8 experiments were performed to test the cell proliferation or viability of Y79 cells with the impact of SAM and HLY78 on Y79 cell proliferation. (B) RT-PCR was employed to test the effect of SAM and HLY78 on the expression of mRNA level of Wnt2/ $\beta$ -catenin. (C) The Wnt2/ $\beta$ -catenin and cleaved caspase 3/caspase 3 expressions were determined by western blot. (D) RT-PCR was employed to test the expression of mRNA level of related genes. nsP > 0.05, \*P < 0.05, \*\*P < 0.01, \*\*\*P < 0.001, \*\*\*\*P < 0.0001 (vs. control or low dose administration group). CCK8, Cell counting kit-8; SAM, S-adenosylmethionine.



TUNEL assay results revealed a greater dose-dependent increase in the rate of apoptosis in the SAM-treated group compared to the control group, which exhibited typical apoptotic features (Figures 3b–e;  $P < 0.01$ ).

To understand more precisely the specific time points of the cell cycle in which SAM is mainly involved, we used flow cytometry to study its cell cycle distribution. Our results showed that the SAM-treated group exhibited a higher proportion of Y79 cells in the G1 phase (Y79: 48.70%–57.80%;  $P < 0.01$ ) compared to the untreated control group, while the proportion of cells in the S phase (Y79: 34.00%–21.20%) was significantly reduced ( $P < 0.001$ ). Between the two SAM treatment groups, there was no significant difference in the low dose administration group (1 mM) compared to the high dose administration group (2 mM), which was not dose-dependent (Figures 3c–f;  $P < 0.05$ ).

### 3.3. SAM inactivated the Wnt2/β-catenin signaling pathway and related gene expression

To explore the mechanism by which SAM acts on Y79 cells, RT-PCR and Western blot analyses were conducted. RT-PCR was shown that it's lower for cell proliferation gene Ki67, metastasis-related genes mmp-2, mmp-9, cell cycle-related genes P21, TP53, vascular endothelial factor (VEGF), transforming growth factor (TGF)-β compared to control group, while apoptosis-related genes caspase3, bax, bcl-2 were higher (Figures 4b and c,  $P < 0.05$ ). SAM treatment significantly reduced the mRNA levels of Wnt2, β-catenin, c-MYC, cyclin D, and c-JUN compared to the control group. Conversely, the mRNA level of AXIN1 and GSK-3β was enhanced (Figure 4a,  $P < 0.05$ ). Furthermore, Western blot analysis demonstrated a noticeable downregulation of Wnt2 and β-catenin proteins after SAM treatment compared to the control group (Figures 4d and e,  $P < 0.05$ ). These findings suggest that SAM may inhibit the activation of the Wnt2/β-catenin signaling pathway.

### 3.4 The Wnt2/β-catenin agonist HLY78 attenuated the oncogenic effect of SAM on retinoblastoma

To further show that SAM may exert its oncostatic effects on retinoblastoma through the Wnt2/β-catenin signaling pathway, we used the Wnt2/β-catenin agonist, HLY78 (1 μM), which acted on retinoblastoma cell Y79 compared with control-0mM-SAM-1mM and SAM-2mM group. Four groups: (1) control-0mM; (2) HLY78; (3) AM-1mM + HLY78; (4) SAM-2mM + HLY78 were detected to be expressed at the level of cell proliferation, related genes' mRNAs and proteins. The results showed that the addition of agonist HLY78 treatment significantly promoted cell proliferation (Figure 5a;  $P < 0.01$ ). Meanwhile, RT-PCR and protein blotting were applied to detect the Wnt2/β-catenin signaling pathway and its related

genes. The results showed that HLY78 significantly increased the expression levels of retinoblastoma Wnt2, β-catenin, C-MYC, C-JUN, cycD, Ki67, and bcl2, and decreased the expression levels of Axin1, GSK-3β, caspase3, and bax ( $P < 0.05$  compared with control-0mM group, Figures 5b–d). However, the oncogenic effect of SAM on retinoblastoma was not completely lost even after the addition of the agonist HLY78. The effect of HLY78 in attenuating the cancer inhibitory effect decreased as the concentration of SAM increased ( $P < 0.05$  compared with the HLY78 group). These results suggested that the oncogenic effect of SAM on retinoblastoma could be attenuated by activating the Wnt2/β-catenin signaling pathway.

### 3.5. SAM attenuated Y79 cell proliferation and growth *in vivo*

To further confirm *in vitro* experiments, *in vivo* experiments were conducted to investigate the impact of SAM on the growth of Y79 cells (Figure 6a). The data indicates that following treatment with SAM, compared to the control group, the experimental group exhibited a significant reduction in tumor volume, and a significant increase in the change in body weight compared to the initial weight of the nude mice before euthanasia (Figures 6b–d,  $P < 0.05$ ). Overall, these data confirm that SAM inhibits the growth and proliferation of Y79 cells. In addition, the detection of liver and kidney function indexes in the serum of nude mice: alanine aminotransferase, aspartate transaminase, creatinine, and urea showed no statistically significant difference between the control group and the experiment, suggesting that the drug is not toxic to the liver and kidney (Figure 6g,  $P > 0.05$ ). Next, we utilized immunohistochemistry to evaluate the expression of Ki67 in tumor tissues. As shown in the figure, compared with the negative control group, the average areas with positive Ki67 staining all showed a decreasing trend (Figures 6e and f,  $P < 0.05$ ). It further verified the results of our *in vitro* experiments.

## 4. Discussion

Retinoblastoma is the predominant primary intraocular tumor in kids and its low incidence still causes significant distress for affected families. Current treatments often yield unsatisfactory outcomes, largely due to the high risk of children losing their eyes to the tumor. In contrast to conventional radiotherapy, SAM, a natural compound found in the human body and commonly used as a nutritional supplement, has shown promise in clinical use for treating conditions such as depression, joint disorders, fibromyalgia, liver disease, and migraines (Galizia et al. 2016). Given its natural origin and minimal adverse effects, SAM exhibits potent anti-tumor activity and has emerged as a potential new anti-cancer

drug for children with retinoblastoma. As awareness of retinoblastoma grows, an increasing number of drugs are being discovered and researched for their efficacy in clinical settings. Our findings demonstrate that SAM inhibits retinoblastoma development in a dose-dependent and time-dependent manner. Further investigation into its mechanism of action revealed its potential in attenuating the Wnt2/ $\beta$ -catenin signaling pathway, suggesting that SAM holds promise for using as a therapeutic agent for retinoblastoma.

This study aimed to explore the mechanism underlying the impact of SAM on the proliferation, apoptosis, and cell cycle of retinoblastoma. SAM has been demonstrated to be an effective therapeutic approach for diverse conditions, including depression and liver disease, without causing serious side effects, unlike common chemotherapeutic drugs. Therefore, SAM has the potential to become a new anti-tumor drug. It is well-known that SAM has an antiproliferative effect. The first step in this study was to determine the optimal effective concentration of SAM against the retinoblastoma cell line Y79, which was found to be 1–2 mM after a 48-h treatment. Flow cytometry analysis revealed a significant reduction of cancer cells in the S phase and an accumulation of cells in the G1 phase among the treated cells. Targeting the cell cycle machinery has shown promise in cancer therapy. In recent years, the Wnt2/ $\beta$ -catenin pathway has been activated in various types of tumor cells, contributing to cell proliferation, apoptosis, differentiation, metastasis, and infiltration. Inhibiting the activated Wnt2/ $\beta$ -catenin signaling pathway can lead to programmed cell death and growth inhibition in various tumor cells. Based on these findings, the Wnt2/ $\beta$ -catenin pathway may serve as a promising marker and therapeutic target for different types of malignancies. It is worth noting that our results demonstrated that SAM significantly inhibited the protein levels of Wnt2 and  $\beta$ -catenin, and decreased the mRNA expression of GSK-3 $\beta$  and AXIN1, which are major downstream factors associated with the Wnt2/ $\beta$ -catenin signaling pathway. Our RT-PCR analysis demonstrated that SAM reduced the mRNA expression levels of Wnt2/ $\beta$ -catenin and its downstream target genes, including C-MYC, C-JUN, and cycD. Additionally, SAM decreased the expression levels of cell cycle-related genes P21 and TP53, as well as vascular endothelial factors VEGF and TGF- $\beta$ . This further supports the notion that SAM may play an anticancer role in retinoblastoma by inhibiting the Wnt2/ $\beta$ -catenin signaling pathway. Interestingly, there were statistically significant differences between the SAM-1mM and SAM-2mM groups compared to the control-0mM group, but there were no significant differences in some genes (e.g., Wnt2,  $\beta$ -catenin, cycD, c-JUN, c-MYC, bcl2, mmp2, mmp9, Ki67, etc.) between the SAM-1mM and SAM-2mM groups, which suggests that by reaching

the dose administered to the low dose group, (it seems) the saturating administered dose is reached, so further increase in the administered dose does not increase the actual effect of the administered dose. Furthermore, in our experimental study using nude mice, we observed a significant reduction in tumor weight and volume during the course of SAM treatment. Biochemical indicators related to blood from the eyeballs of nude mice after tumor excision indicated that the drug does not cause liver or kidney toxicity. Immunohistochemical analysis also indicated a reduction in the expression levels of Ki67 after SAM treatment, which is consistent with our *in vitro* experimental results. The Wnt/ $\beta$ -catenin pathway agonist HLY78 also re-validated that SAM exerted its anticancer effects in Y79 by inhibiting the Wnt2/ $\beta$ -catenin signaling pathway, both at the protein level and at the mRNA level, after treating Y79 cells for 48 h. In conclusion, this study provides the initial evidence indicating that SAM has the potential to inhibit the growth, apoptosis, and cell cycle characteristics of retinoblastoma by interfering with the Wnt2/ $\beta$ -catenin signaling pathway.

## Acknowledgments

Thanks to my teachers and lab friends for their help.

## Statements and Declarations

## Competing Interests

The authors declare no conflict of interest regarding the publication of this manuscript.

## Author Contributions

Shen Hong designed the study and guided the interpretation of the results. Mushi Liu performed the experiments, analyzed the data, and drafted the manuscript. Youchaou Mobet revised and edited the manuscript. All authors read and approved the final version of the manuscript.

## Ethics Statement

This study was conducted following ethical guidelines and was approved by the Experimental Animal Centre of South China University of Technology (Ethics approval number: 2023105).

## Funding

No funding was received for conducting this study.



## References

- Bai QL, Hu CW, Wang XR et al (2017) Mir-616 promotes proliferation and inhibits apoptosis in glioma cells by suppressing expression of Sox7 via the Wnt signaling pathway. *Eur Rev Med Pharmacol Sci* 21:5630–5637. [https://doi.org/10.26355/eurrev\\_201712\\_14006](https://doi.org/10.26355/eurrev_201712_14006)
- Dimaras H, Corson TW, Cobrinik D et al (2015) Retinoblastoma. *Nat Rev Dis Primers* 1:15021. <https://doi.org/10.1038/nrdp.2015.21>
- Galizia I, Oldani L, Macritchie K et al (2016) S-adenosyl methionine (same) for depression in adults. *Cochrane Database Syst Rev* 10:CD011286. <https://doi.org/10.1002/14651858.CD011286.pub2>
- Hayashi T, Teruya T, Chaleckis R et al (2018) S-adenosylmethionine synthetase is required for cell growth, maintenance of G0 phase, and termination of quiescence in fission yeast. *iScience* 5:38–51. <https://doi.org/10.1016/j.isci.2018.06.011>
- He L, Zhou H, Zeng Z et al (2019) Wnt/B-catenin signaling cascade: A promising target for glioma therapy. *J Cell Physiol* 3:2217–2228. <https://doi.org/10.1002/jcp.27186>
- Kruglova MP, Ivanov AV, Virus ED et al (2021) Urine S-adenosylmethionine are related to degree of renal insufficiency in patients with chronic kidney disease. *Lab Med* 52:47–56. <https://doi.org/10.1093/labmed/lmaa034>
- Liu Y, Bi T, Yuan F et al (2020) S-adenosylmethionine induces apoptosis and cycle arrest of gallbladder carcinoma cells by suppression of Jak2/Stat3 pathways. *Naunyn Schmiedeberg's Arch Pharmacol* 393:2507–2515. <https://doi.org/10.1007/s00210-020-01858-6>
- Lu Y, Yang Y, Kang Z et al (2020) High-dose S-adenosylmethionine combined with ursodeoxycholic acid is more suitable for the treatment of cholestatic liver disease. *Int J Clin Exp Med* 13:7365–7371.
- Luo Y, Zhou C, He F et al (2022) Contemporary update of retinoblastoma in China: Three-decade changes in epidemiology, clinical features, treatments, and outcomes. *Am J Ophthalmol* 236:193–203. <https://doi.org/10.1016/j.ajo.2021.09.026>
- Mahmood N, Arakelian A, Cheishvili D et al (2020) S-adenosylmethionine in combination with decitabine shows enhanced anti-cancer effects in repressing breast cancer growth and metastasis. *J Cell Mol Med* 24:10322–10337. <https://doi.org/10.1111/jcmm.15642>
- Parashar S, Cheishvili D, Arakelian A et al (2015) S-adenosylmethionine blocks osteosarcoma cells proliferation and invasion in vitro and tumor metastasis in vivo: Therapeutic and diagnostic clinical applications. *Cancer Med* 4:732–744. <https://doi.org/10.1002/cam4.386>
- Pascual-Pasto G, Bazan-Peregrino M, Olaciregui NG et al. (2019) Therapeutic targeting of the Rb1 Pathway in retinoblastoma with the oncolytic adenovirus Vcn-01. *Sci Transl Med* 11:eaat9321. <https://doi.org/10.1126/scitranslmed.aat9321>
- Perugorria MJ, Olaizola P, Labiano I et al (2019) Wnt-beta-catenin signalling in liver development, health and disease. *Nat Rev Gastroenterol Hepatol* 16:121–136. <https://doi.org/10.1038/s41575-018-0075-9>
- Singh V, Walter V, Elcheva I et al (2023) Global role of Igf2bp1 in controlling the expression of Wnt/B-Catenin-regulated genes in colorectal cancer cells. *Front Cell Dev Biol* 11:1236356. <https://doi.org/10.3389/fcell.2023.1236356>
- Spitzner M, Emons G, Schütz KB et al (2021) Inhibition of Wnt/β-catenin signaling sensitizes esophageal cancer cells to chemoradiotherapy. *Int J Mol Sci* 22:10301. <https://doi.org/10.3390/ijms221910301>
- Vincenzi B, Russo A, Terenzio A et al (2018) The use of same in chemotherapy-induced liver injury. *Crit Rev Oncol Hematol* 130:70–77. <https://doi.org/10.1016/j.critrevonc.2018.06.019>
- Yan H, Li M, Zhang Z et al (2021) [Analysis of fundus examination results in 8 808 pediatric patients in Northwest China]. *Zhonghua Yan Ke Za Zhi* 10:777–783. <https://doi.org/10.3760/cma.j.cn112142-20201217-00823>
- Zsigrai S, Kalmár A, Nagy ZB et al (2020) S-adenosylmethionine treatment of colorectal cancer cell lines alters DNA methylation, DNA repair and tumor progression-related gene expression. *Cells* 9:1864. <https://doi.org/10.3390/cells9081864>